Supporting information for: CO_2 Adsorption in Fe_2(dobdc): A Classical Force Field Parameterized from Quantum Mechanical Calculations

Joshua Borycz,[†,‖] Li-Chiang Lin,[‡,‖] Eric D. Bloch,[‡] Jihan Kim,[¶] Allison L. Dzubak,[†] Rémi Maurice,[†,§] David Semrouni,[†] Kyuho Lee,[‡] Berend Smit,[*,‡] and Laura Gagliardi[*,†]

Department of Chemistry, Supercomputing Institute, and Chemical Theory Center, University of Minnesota, 207 Pleasant Street SE, Minneapolis, Minnesota 55455-0431, USA, Department of Chemical and Biomolecular Engineering and Chemistry, University of California, Berkeley, California 94720-1462, USA, Department of Chemical and Biomolecular Engineering, Korea Advanced Institute of Science and Technology, 291 Daehak-ro Yuseonggu, Korea 305-710, and SUBATECH, UMR CNRS 6457, IN2P3/EMN Nantes/Université de Nantes, 4 rue Alfred Kastler, BP20722, 44307 Nantes Cédex 3, France

E-mail: berend-smit@berkeley.edu; gagliard@umn.edu

[*]To whom correspondence should be addressed
[†]University of Minnesota
[‡]University of California, Berkeley
[¶]Korea Advanced Institute of Science and Technology
[§]IN2P3/EMN Nantes/Université de Nantes
[‖]These authors contributed equally to this work.

S1 Clusters

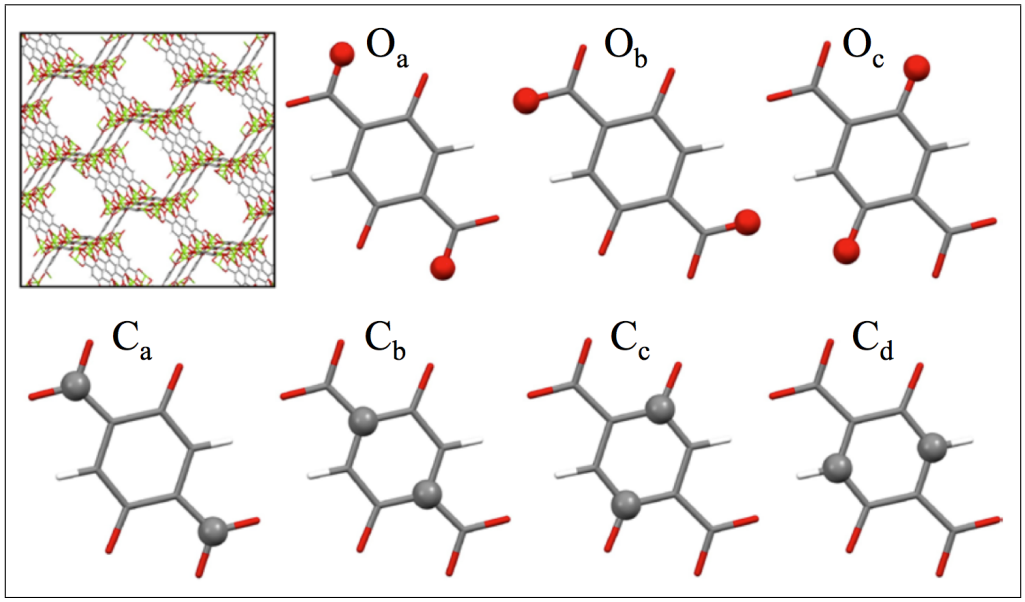

Figure S1: Different oxygen and carbon types within MOF-74. This figure is reproduced from the SI of ref S1.

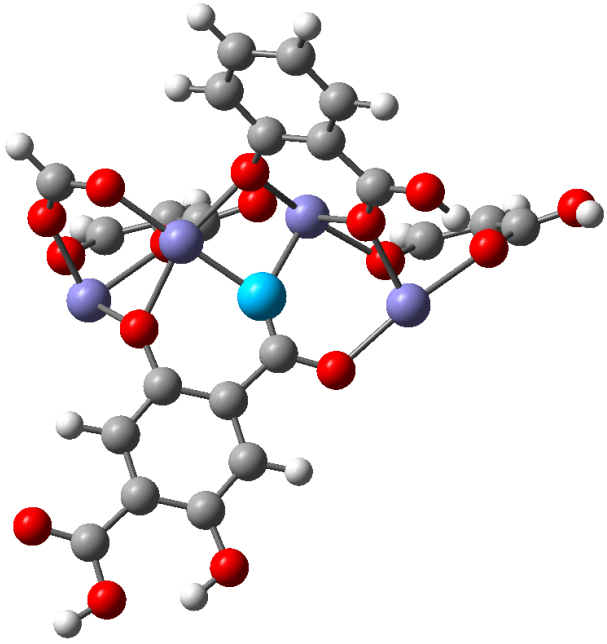

Figure S2: Cluster designed to represent the O_a atom and its local environment in Fe-MOF-74. The O_a atom is light blue, iron is dark blue, oxygen is red, carbon is grey, and hydrogen is white.

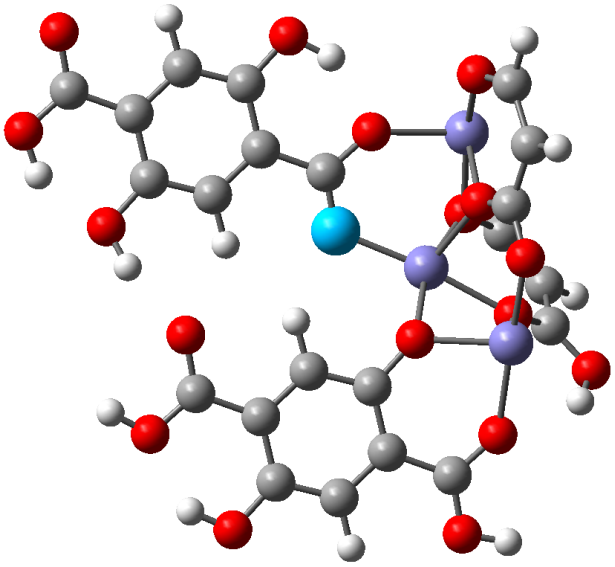

Figure S3: Cluster designed to represent the O_b atom and its local environment in Fe-MOF-74. The O_a atom is light blue, iron is dark blue, oxygen is red, carbon is grey, and hydrogen is white.

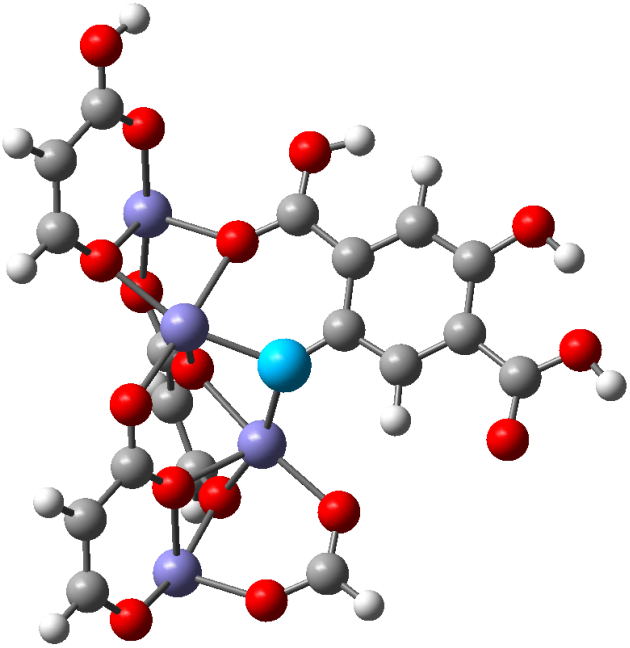

Figure S4: Cluster designed to represent the O_c atom and its local environment in Fe-MOF-74. The O_a atom is light blue, iron is dark blue, oxygen is red, carbon is grey, and hydrogen is white.

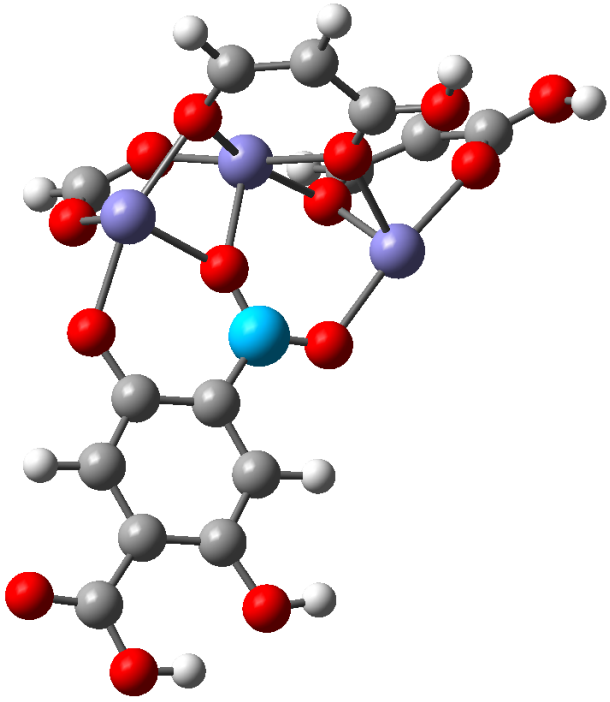

Figure S5: Cluster designed to represent the C_a atom and its local environment in Fe-MOF-74. The O_a atom is light blue, iron is dark blue, oxygen is red, carbon is grey, and hydrogen is white.

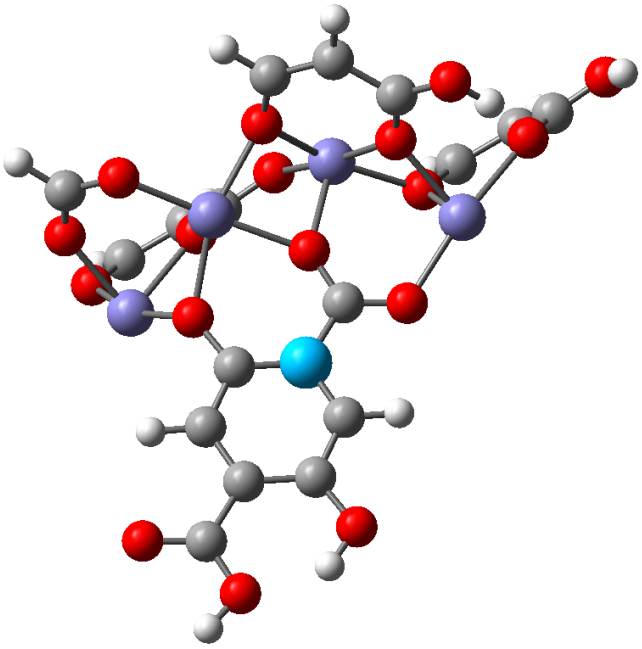

Figure S6: Cluster designed to represent the C_b atom and its local environment in Fe-MOF-74. The O_a atom is light blue, iron is dark blue, oxygen is red, carbon is grey, and hydrogen is white.

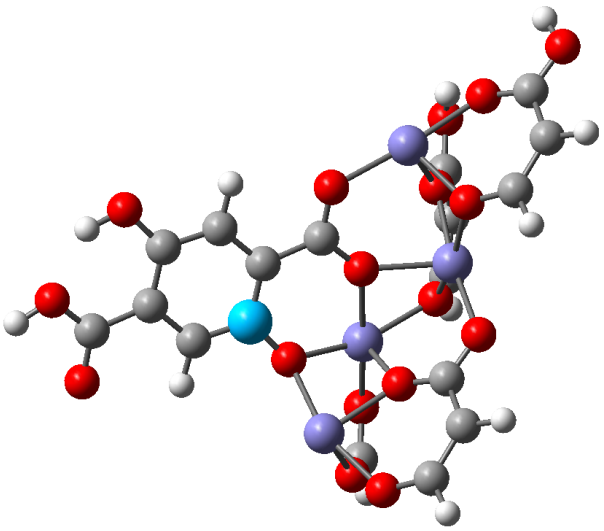

Figure S7: Cluster designed to represent the C_c atom and its local environment in Fe-MOF-74. The O_a atom is light blue, iron is dark blue, oxygen is red, carbon is grey, and hydrogen is white.

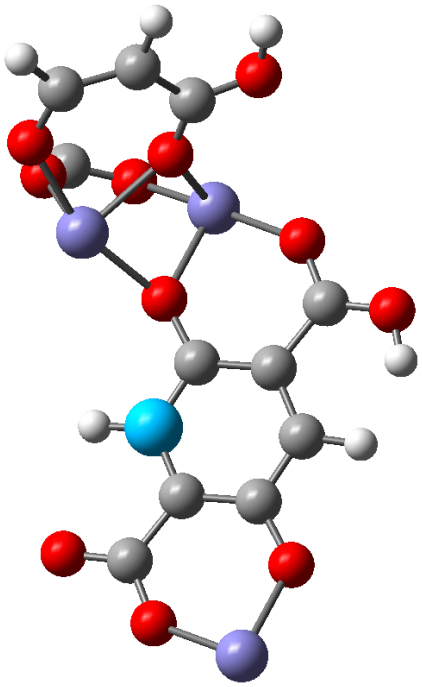

Figure S8: Cluster designed to represent the C_d atom and its local environment in Fe-MOF-74. The O_a atom is light blue, iron is dark blue, oxygen is red, carbon is grey, and hydrogen is white.

S2 Counterpoise Correction

The counterpoise correction requires that the basis functions of the ghost atoms of the other molecule must be included in each of the monomer calculations. Thus, in the calculation of the E_{MOF} term the basis functions for CO_2 must be included and vice versa. This corrects the tendency to overestimate binding in interaction energy calculations due to the asymmetry of the basis set sizes. The form of the counterpoise correction E^{CP} and the the counterpoise corrected binding energy $E_{\mathrm{int}}^{\mathrm{CP}}$ are provided as eq S1. Note that since the MOF fragments and the CO_2 molecule are considered rigid, $E_{\mathrm{int}}^{\mathrm{CP}}$ has a simple expression, and that only three computed energies are required.

$$\begin{aligned} E_{\mathrm{int}} &= E(AB) - [E(A) + E(B)] \\ E^{\mathrm{CP}} &= E(A)_A - E(A)_{AB} + E(B)_B - E(B)_{AB} \\ E_{\mathrm{int}}^{\mathrm{CP}} &= E(AB) - [E(A)_{AB} + E(B)_{AB}] \end{aligned} \tag{S1}$$

where $E(A)$ is the energy of monomer A, $E(A)_A$ is the energy of A with the basis of A, and $E(A)_{AB}$ is the energy of A with the basis of AB. The $E(B)$ terms match correspondingly.

S3 NEMO Equations

$$E_{\mathrm{elect}} = \sum_i^{N_A}\sum_j^{N_B} T^{ij}(q^i q^j) + T_\alpha^{ij}(q^i \mu_\alpha^j - \mu_\alpha^i q^j) - T_{\alpha\beta}^{ij}(\mu_\alpha^i \mu_\beta^j) + \cdots \tag{S2}$$

$$\begin{aligned} E_{\mathrm{ind}} &= -\frac{1}{2}\sum_i^{N_A}\sum_j^{N_B} \mu_\alpha^{j,\mathrm{ind}} F_{\alpha'}^i(\mathbf{j}) + \mu_\alpha^{i,\mathrm{ind}} F_{\alpha'}^j(\mathbf{i}) \\ &= -\frac{1}{2}\sum_i^{N_A}\sum_j^{N_B} F_\alpha^i(\mathbf{j})\alpha_{\alpha\alpha'}^j F_{\alpha'}^i(\mathbf{j}) + F_\alpha^j(\mathbf{i})\alpha_{\alpha\alpha'}^i F_{\alpha'}^j(\mathbf{i}) \\ &= -\frac{1}{2}\sum_i^{N_A}\sum_j^{N_B} (q^i T_\alpha^{ij} - \mu_\beta^i T_{\alpha\beta}^{ij} + \cdots)\alpha_{\alpha\alpha'}^j (q^i T_{\alpha'}^{ij} - \mu_{\beta'}^i T_{\alpha'\beta'}^{ij} + \cdots) \\ &\quad + (q^j T_\alpha^{ij} - \mu_\beta^j T_{\alpha\beta}^{ij} + \cdots)\alpha_{\alpha\alpha'}^i (q^j T_{\alpha'}^{ij} - \mu_{\beta'}^j T_{\alpha'\beta'}^{ij} + \cdots) \end{aligned} \tag{S3}$$

$$E_{\text{disp}} = \sum_{i}^{N_A} \sum_{j}^{N_B} \frac{\varepsilon E_{12}}{4} \alpha^{i}_{\alpha\beta} \alpha^{j}_{\gamma\delta} T^{ij}_{\alpha\gamma} T^{ij}_{\beta\gamma} \tag{S4}$$

$$T^{(n)}_{\alpha\beta\ldots\nu} = \frac{1}{4\pi\varepsilon_0} \nabla_\alpha \nabla_\beta \ldots \nabla_\nu \frac{1}{r_{ij}} \tag{S5}$$

The charge is represented by q, μ represents the dipole moment (μ^{ind} is the induced dipole), and A and B represent the two molecules interacting. The i and j terms are the atomic sites of molecules A and B, $\mathbf{i}$ and $\mathbf{j}$ are the vector positions of atoms i and j, and N_A and N_B represent the total number of atoms in systems A and B. The induction term is modeled using mutually induced point-dipole moments and the dispersion is modeled considering the interaction of the components of the isotropic polarizabilities represented by $\alpha^{i}_{\alpha\beta}$ and $\alpha^{j}_{\alpha\beta}$. In the induction term, $F^{i}_{\alpha}(\mathbf{j}) = (q^{i} T^{ij}_{\alpha} - \mu^{i}_{\beta} T^{ij}_{\alpha\beta} + \ldots)$ can be considered the component on the α axis of the electric field on atom j due to atom i calculated with the electrostatic contribution truncated at quadrupoles. The Greek subscripts refer to different cartesian directions, and the α and α' subscripts express a rotation that transforms the cartesian direction α to α'. E_{12} is the average molecular excitation energy. $\mathbf{T}$ is the interaction tensor. The general form of the interaction tensor elements are reported as eq S5. Term (n) specifies the number of subscripts and ∇_α is the gradient with respect to position along some cartesian direction α. Note that the quadrupole interaction terms are not shown for clarity. No damping function was used.

S4 LoProp Charges Used in the Simulations

Table S1: LoProp charges for Fe-MOF-74 and Mg-MOF-74 computed with ROMP2 using the clusters provided in Figures S2-S8.

Atom	Charge	
	Fe-MOF-74	Mg-MOF-74[a]
Metal	1.5118	1.5637
O_a	-0.7544	-0.7654
O_b	-0.7043	-0.7088
O_c	-0.8022	-0.8328
C_a	0.6114	0.4820
C_b	-0.1385	-0.1354
C_c	0.2279	0.1890
C_d	-0.1606	-0.1814
H	0.2089	0.3891

[a]Taken from ref S1.

S5 Unit Cells

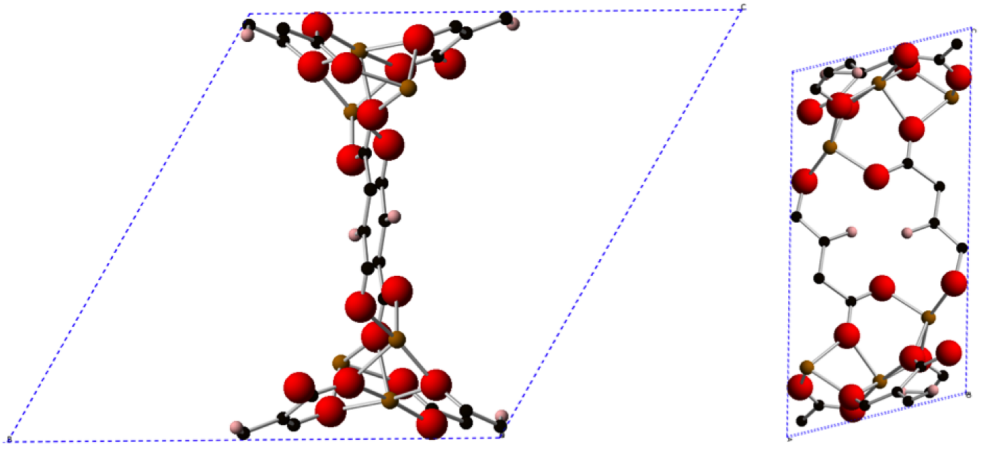

Figure S9: Primitive cell of Fe-MOF-74, which contains 54 atoms. The Fe(II) ions are brown, oxygen atoms are red, carbon atoms are black, and hydrogen atoms are pink.

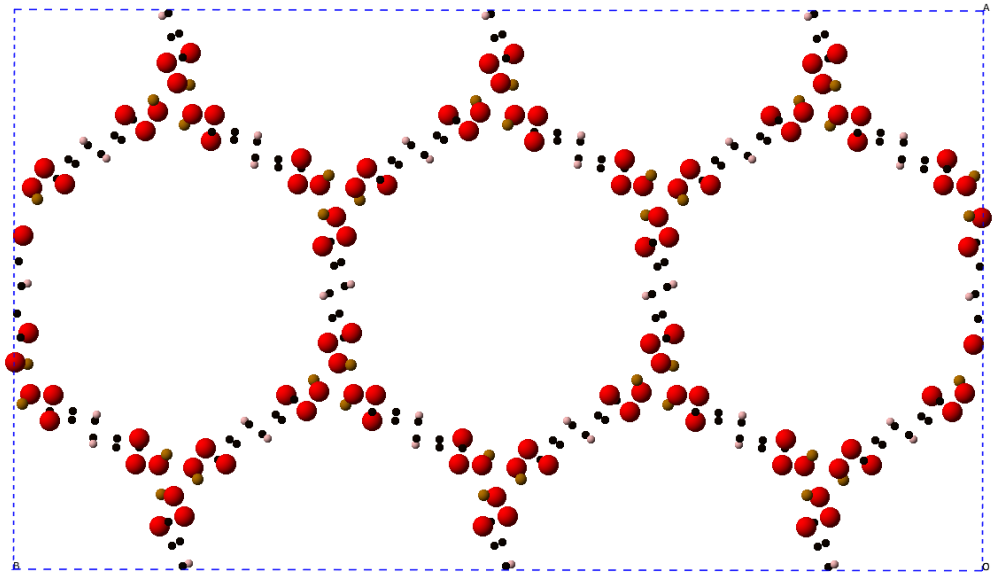

Figure S10: Orthogonalized unit cell containing 324 atoms that was used in the GCMC simulations. Note that the simulation box was a $1 \times 1 \times 4$ supercell.

Table S2: Lattice parameters of the orthogonalized unit cell used in the GCMC simulations. The simulation box had a lattice vector in the c direction of length 27.8296 Å.

a (Å)	b (Å)	c (Å)	α	β	γ
45.7985	26.4418	6.9574	90	90	90

S6 Scaling Factor

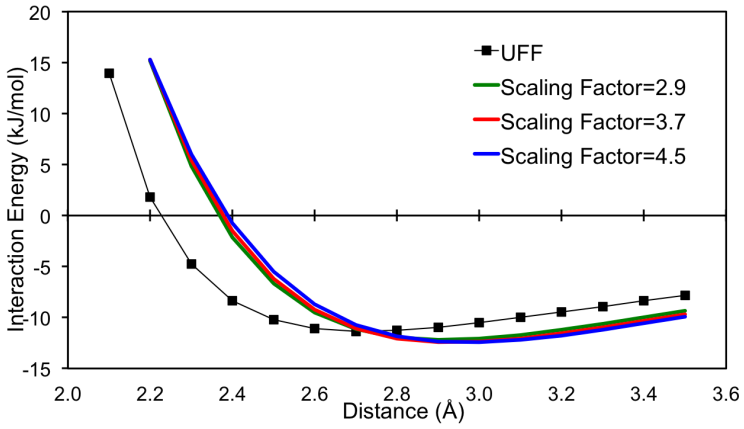

Figure S11: Three scaling factors are compared to findings from UFF for the Fe-MOF-74 cluster/CO_2 interaction.

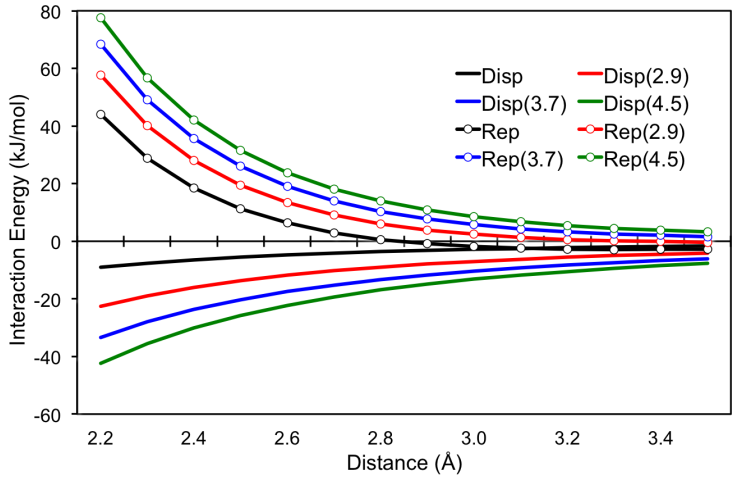

Figure S12: Dispersion and repulsion curves from the NEMO decomposition of the ROMP2 PEC of the 60-atom cluster from Fe-MOF-74 interacting with CO_2. The original values from the calculation and the curves produced with three different scaling factors are provided.

S7 Isosteric Heat of Adsorption

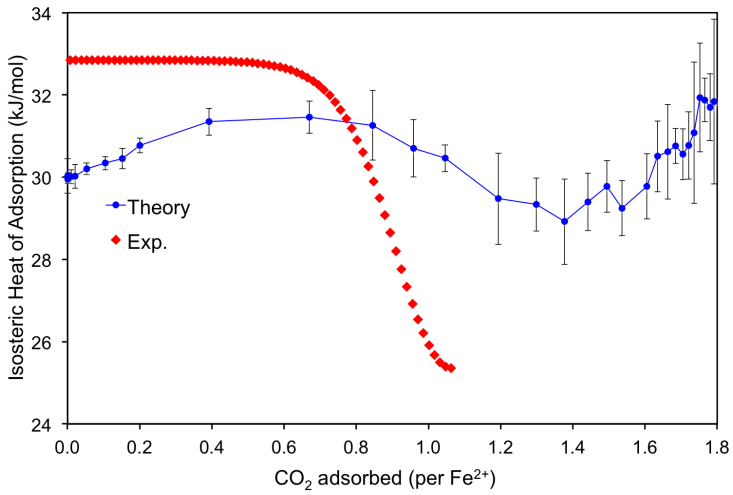

Figure S13: Experimental and theoretical isosteric heat of adsorption curves.

References

(S1) Dzubak, A. L.; Lin, L.-C.; Kim, J.; Swisher, J. A.; Poloni, R.; Maximoff, S. N.; Smit, B.; Gagliardi, L. *Ab initio* Carbon Capture in Open-Site Metal-Organic Frameworks. *Nat. Chem.* **2012**, *4*, 810–816.